



University of HUDDERSFIELD

University of Huddersfield Repository

Vishnyakov, Vladimir, Crisan, O., Dobrosz, P. and Colligon, John

Ion sputter-deposition and in-air crystallisation of Cr₂AlC films

Original Citation

Vishnyakov, Vladimir, Crisan, O., Dobrosz, P. and Colligon, John (2014) Ion sputter-deposition and in-air crystallisation of Cr₂AlC films. *Vacuum*, 100. pp. 61-65. ISSN 0042-207X

This version is available at <http://eprints.hud.ac.uk/21984/>

The University Repository is a digital collection of the research output of the University, available on Open Access. Copyright and Moral Rights for the items on this site are retained by the individual author and/or other copyright owners. Users may access full items free of charge; copies of full text items generally can be reproduced, displayed or performed and given to third parties in any format or medium for personal research or study, educational or not-for-profit purposes without prior permission or charge, provided:

- The authors, title and full bibliographic details is credited in any copy;
- A hyperlink and/or URL is included for the original metadata page; and
- The content is not changed in any way.

For more information, including our policy and submission procedure, please contact the Repository Team at: E.mailbox@hud.ac.uk.

<http://eprints.hud.ac.uk/>

Ion sputter-deposition and in-air crystallisation of Cr₂AlC films

V. Vishnyakov⁺, O.Crisan, P.Dobrosz and J.S. Colligon

School of Computing and Engineering, The University of Huddersfield, Queensgate,
Huddersfield H1 3DH

(Formerly Manchester Metropolitan University, Manchester M1 5GD, UK)

Ternary alloys of composition close to Cr₂AlC have been deposited by ion beam sputtering onto unheated and heated to 380 °C Si substrates. As-deposited films have very small crystallites at around 7 nm. Annealing of the film in air at 700°C leads to crystallite growth to 32.3 nm. Crystallisation also can be achieved by annealing in air but there is also partial oxidation of the film surface to the depth of approximately 120 nm, which represents an oxide layer less than 5% of the total film thickness. There is an increase of lattice size along the c-axis during crystallisation in air, which can indicate small incorporation of oxygen. Film structure and crystallisation have also been analysed by Raman spectroscopy. This is the first time that changes in Raman spectra in Cr₂AlC have been correlated with crystallite size and it was observed that MAX-phase related peaks become sharper for bigger crystallites.

Keywords: Ternary carbides; ion sputtering; annealing; crystallisation; XRD analysis; WDX analysis, Raman spectrascopy

⁺ Corresponding author: tel. +44 (0)161 247 1201, email v.vishnyakov@hud.ac.uk

It is well known that chromium containing materials have exceptional engineering properties. The materials excel in high temperature oxidation resistance and have been used as protective coatings for decades as can be seen in some early work and references therein [1, 2]. A few decades ago Nowotny and co-workers achieved synthesis of a large class of ternary carbides and nitrides with quite unique properties such as lamination of atoms on the nanoscale [3, 4]. The resurgence of work on those materials in the last decade is closely linked to Barsoum's early work [5] and the field has been highlighted again in the latest reviews [6-9]. The general formula of the nanolaminated materials in many cases can be presented as $M_{n+1}AX_n$, where $n=1, 2, \text{ or } 3$; M is a transition metal, A is an A-group element, and X is C or N. The name "MAX phases" for the crystalline arrangements was coined by Barsoum [6]. One significant property which unites all MAX phases is their nanolaminated structure. The majority of bulk MAX phases require high, in excess of 1200 °C, temperatures for synthesis and synthesis of pure phases is nontrivial due to formation of competing binary compounds. The first synthesis by Physical Vapour Deposition (PVD) onto single-crystal substrates was reported in 2002 by Palmquist *et al.* [10]. Since then about 70 compounds have now been synthesised. [8, 9].

Retention of mechanical properties and high oxidation resistance of many MAX phases at high temperatures has made synthesis of thin film MAX phase materials an important research area. A major research challenge is to lower the formation temperature of MAX phases and to determine if the desired material properties can be achieved either as MAX phase or as material with MAX composition only. For the 211 phases Cr_2AlC , V_2AlC , Cr_2GeC , and V_2GeC it is possible to form fully-developed crystalline structures at around 500-700 °C [11-17]. The Ti-containing 211 phases Ti_2AlC and Ti_2GeC , however, were grown at temperatures of order 700 °C [18, 19] and only recently the Ti_3SiC_2 was grown at 650 °C on a non-epitaxial substrate [20].

Thin films of Cr_2AlC composition have been synthesized using magnetron sputtering techniques from elemental targets [6,7] and from compound targets [8-10]. In particular, using dc magnetron sputtering from a compound target, Walter *et al.* [8] have reported formation of single-phase Cr_2AlC thin films on stainless steel substrates heated at temperatures around 650°C. However it is clear that, from an industrial viewpoint, deposition at high temperatures is less attractive than deposition without additional heating (cold deposition) followed by annealing to promote crystallisation and true MAX phase state.

Rapid thermal annealing has been successfully shown to create a MAX phase after deposition at low temperature [21]. One also needs to bear in mind that "cold" PVD while not achieving a nanolaminated atomic structure would create an almost amorphous bonding network. The material with this structure will have different properties than that of the true MAX phase. The questions arise whether the state of Cr_2AlC is important for some applications and, indeed, is it important for some applications to have crystalline material in the first place? This communication presents the first set of data to address the above questions.

For the Cr_2AlC thin film deposition a dual ion-beam system was used (base pressure 2×10^{-6} mbar) which is described in detail elsewhere [22]. In brief, the composite target was sputtered by 1.2 keV Ar^+ ions from a 3 inch diameter Kaufman ion source. The sputtering composite target was made out of elemental Cr, graphite and Al sheets. The relative elemental target sputtered areas are fully adjustable in order to finely tune the sample to the desired chemical composition. Prior to the deposition the composite target was Ar^+ ion sputter-cleaned for at least 30 min.

The thin films were deposited onto Si (100) and polished M42 high speed steel substrates in an Ar pressure of 2×10^{-4} mbar. The produced samples are divided in to two categories. In the first category are samples deposited on the substrates without additional substrate heating. Previous measurements show that the substrate in this case reaches approximately 80-100 °C during the first 15 min of the film deposition and then remains at this temperature. To the second category belong samples for which the substrate holder was heated up to 380 °C. Deposition was carried out for 2 hours, which allowed production of films approximately 1.4 μm thick

Post-deposition annealing treatments have been performed *ex situ* (in-air) or in a separate vacuum furnace with base pressure 3×10^{-6} mbar. In both cases the temperature was ramped at a rate of around 40-50 K/min. Samples were then kept for 20 min at the stated annealing temperature and the heating was switched off.

The chemical composition was measured by Energy-Dispersive X-ray Spectroscopy (EDX) and Wave-Dispersive X-Ray Spectroscopy (WDX). The structure and morphology have been investigated using grazing incidence X-ray diffraction (GIXRD) and scanning electron microscopy (SEM). A Philips X'pert 20 diffractometer has been used for the XRD studies, while SEM images were obtained using a Carl Zeiss Supra 40 VP FEG (field-emission gun) scanning electron microscope with EDAX EDX and WDX detectors. While both EDX and WDX give similar information about the chemical composition of the sample, WDX has the advantage in high energy resolution and quantifies quite accurately the content of oxygen in the sample with Cr.

Raman spectra were collected in the backscattering configuration using a Renishaw inVia spectrometer with air-cooled CCD array detector in the backscattering configuration. An Ar laser (514 nm) with incident power of ~ 1.7 mW was focused on a spot size of ~ 2 μm on the surface. The spectra were fitted using a multi-peak Lorentzian + Gaussian fitting of all experimental peaks observed. The resolution of the obtained linewidths and peak positions is within 2 cm^{-1} .

The surface of near stoichiometric Cr_2AlC thin films deposited without additional heating is in general smooth with few hillocks and does not change significantly after annealing at 700 °C. This glassy-like appearance is a first indication of the possible close to amorphous state of the as-deposited film which is later confirmed by XRD.

In principle the chemical composition (Cr, Al and C content) of the films can be found by EDX. Figure 1a shows typical EDX spectra for the samples. In this case quantification is done on CrK, AlK and CK lines. The samples deposited from the same sputtering target onto the unheated substrate and onto the substrate heated to 380°C show almost the same composition, within the error range of the experimental EDX technique. For the sample in Fig.1 quantitative analysis shows that the Cr:Al:C relative composition is close to 52:25:23 at.%.

A problem for EDX analysis arises as the oxygen OK line sits in the same range as the CrL lines, in fact in-between two main L lines. The EDX detector has around 90 eV (FWHM) resolution at this energy and the software, as a black box, can do the line deconvolution, which is hardly can be deemed satisfactory. The solution in this case is to use the WDX spectrometer, which, as can be seen on Fig.2, produces well-resolved lines in this region. Deconvolution of the spectra, with CasaXPS software in our case, allows singling out the oxygen line.

After annealing in air the area of the oxygen peak significantly increases (see Fig.2) due to some oxidation of the MAX alloy layer. It is possible to utilise a range of electron energies for assessment of the oxide layer thickness and to analyse how oxygen is distributed in the thin film after annealing.

In order to interpret the multi-energy data we have employed the electron interaction modelling program CASINO V2.42 [10]. It was taken, on the basis of X-Ray Photoelectron spectroscopy (data are not presented in the paper), that both Chromium and Aluminium form fully stoichiometric oxides Cr_2O_3 and Al_2O_3 , which makes the oxide layer composition Cr_2AlCO_5 . We have assumed that the X-Ray Collection Efficiency Function for both $\text{CrL}\alpha$ and $\text{OK}\alpha$ is equal, which should be a reasonable approximation as the line energies are very close. The modelling shows that, to satisfy line integral ratios, the oxide layer should be approximately 120 nm thick, which is less than 10% of the whole film thickness. The integral ratio saturation at energies above 10 keV is explained by heavy $\text{CrL}\alpha$ X-ray absorption in the material as X-rays of this energy do not normally escape from a depth above approximately 300 nm.

The grazing incidence theta-2-theta geometry was chosen for the XRD analysis in order to minimize the strong signals arising from the Si(100) Bragg lines. The sample deposited without additional substrate heating appears to be amorphous and even remain amorphous after annealed at 650°C for 20 min (data are not present in the paper). The XRD patterns of the sample deposited onto the heated up to 380 °C substrate, are shown in Fig.3 together with the patterns corresponding to the same sample annealed at 700°C for 30 min in air and in vacuum.

The as-deposited film at elevated temperature (380⁰C) shows a pattern with broad Bragg lines, centred at about 42 degrees (in 2-theta). Usually such patterns are characteristic of a material structure made of small nanograins with topological disorder and amorphous-like structure. The main broad line observed in the pattern can be indexed as belonging to the Cr_2AlC and is mainly the (103) reflection. The situation is rather different in the case of the sample annealed at 700°C for 30 min in air. In this case the XRD pattern presents very sharp, well-defined Bragg lines that are all attributed to the Cr_2AlC . It follows that, in this latter case, the microstructure is formed by larger grains, the film being completely crystallized. In the case of this completely crystallized film, the only phase identified by the XRD pattern analysis is the Cr_2AlC hexagonal structure, with the P63/mmm space group. This finding is in agreement with previous reports [11] on crystallization behaviour of Cr_2AlC . It has been shown by differential scanning calorimetry that the crystallization temperature of the Cr_2AlC is between 670-680°C, a fact that explains the occurrence of the full crystalline structure only after annealing at 700°C. The pattern analysis reveals also presence of crystalline chromium oxide (see later).

A more-detailed XRD pattern is found in the case of a sample annealed at 700⁰C in vacuum. In this case also, the less intense Bragg reflections of (002), (004) and (106) of the hexagonal structure of Cr_2AlC are observable. For this sample, the hexagonal Cr_2AlC is

found to be the main phase observed (more than 95% of the total intensity of the Bragg reflections).

We have applied the Rietveld-type refinement procedure on the XRD patterns in order to obtain with accuracy the phase composition as well as structural parameters such as: lattice parameters, unit cell volume and average grain sizes using the integral breadth method. All the patterns have been fitted using MAUD (the method description can be found for example in [23]) and Datlab [24] programs). These powder diffraction packages, developed for polycrystalline multiple phase materials, allow deconvolution of complex overlapping Bragg peaks, calculation of position and line-width of each individual Bragg reflection and the determination of lattice parameters. For the current communication Datlab has been used for the peak analysis and calculation of lattice parameters in the as-deposited and annealed samples while MAUD was used to determine quantitatively the phase composition in the samples.

As well as the Cr_2AlC hexagonal phase, traces of Cr_2O_3 hexagonal phase have also been identified in the XRD pattern after crystallisation in air. Quantitative analysis based on whole profile fitting show that, in the crystallized-in-air sample, the Cr_2AlC represents 95.5% wt of the sample while the Cr_2O_3 represents 4.5% wt, a finding that is in line the WDX results.

The Bragg peaks of the diagrams have been fitted to a pseudo-Voigt line profile, which accounts for broadening by two mechanisms. The first one is strain-related and would produce a Gaussian profile, and the other is related to the size of the grains and would produce a Lorentzian profile. The full width at half maximum (FWHM) of the Voigt profile (w) is a convolution of the widths of the associated Gaussian and Lorentzian profiles. A simplified pseudo-Voigt profile reads: $pV(x) = (1-\eta)G(x)+\eta L(x)$ where η is the mixing parameter. This parameter, that has values between 0 and 1, is an expression of the Bragg peak asymmetry and represents a quantitative estimation of the Lorentz relative proportion in the Voigt profile. By using the lattice parameters, line-widths and mixing parameters of the assumed pseudo-Voigt profile of the Bragg lines, obtained for each Bragg reflection, we were able to calculate the average crystallographic domain size associated with the average diameter of the grains. The method we used is based on the integral breadth algorithm. The program calculates domain size from input integral breadths of at least two physically broadened (due to the crystallite size) diffraction line profiles.

The results of the fittings are given in Table 1. The lattice parameters which resulted from the fit as well as the unit cell volume are quite close to the values for the bulk Cr_2AlC ($a = 2.86 \text{ \AA}$ and $c=12.82 \text{ \AA}$). Most of the variation is related to c-axis, lengths which decrease upon annealing and become closer to the bulk value; however they remain slightly larger than the value for the bulk samples. It is also evident that, for samples annealed in air at $700 \text{ }^\circ\text{C}$, the lattice parameters remain slightly bigger as compared to the vacuum annealing, which probably indicated that some small amount of oxygen gets into the film bulk and resides interstitially in the lattice. We also can speculate that this oxygen partially suppresses the crystallisation and crystallites are a bit smaller. It is observable that the grain size increases as

a result of deposition at 380 °C to 14.2 nm as compared to deposition onto unheated, cold, substrate.

Both as-deposited and annealed samples were analysed using Raman spectroscopy and the results obtained are shown in Figure 4 and Table 2. The MAX phases are a member of the space group D_{6h}^4 and for the 211 structures there are 4 Raman active optical modes, three of which are Raman active and one which is both Raman and infrared active [25].

The range of the obtained spectrum is between 140 and 2000 cm^{-1} within which three typical areas can be identified. The first area is in the range of 140 – 500 cm^{-1} . In this area there are peaks typical for M_nAX_{n-1} phases (in our case $n = 2$). The second area, 500 – 1000 cm^{-1} , contains mainly peaks due to surface oxides [26] and vibration modes in carbide [27]. The high energy area, 1000 – 2000 cm^{-1} , relates to well known in many carbides carbon-based bonding with two main carbon bonds D and G.

The assignment of the observed Raman peaks have been made in agreement with reported results on Cr_2AlC [25, 27] and Cr_2O_3 [26], respectively. A significant difference is found between an as-deposited and annealed coating for each of the above-mentioned areas. As can be seen from observing the first area in Figure 4, the annealing does not change the total number of visible peaks (1a-1d), however, those peaks are more visible and better defined than those for the as-deposited sample. There is little difference in the peak positions between results for the two analysed samples and those quoted in the literature. Some peaks, such as 1a and 1b for the annealed samples, do overlap and are difficult to distinguish. These peaks are typical for 211 MAX phases and their position is in quite good agreement with literature data. In the second section, for the as-deposited sample 2 peaks are visible (3a and 3b) but after annealing in air a new peak appears (2), the intensity proportion for peaks 3a and 3b reverse and there is significant peak shift. Peak 2 is typical for chromium oxide forming on the surface upon annealing. The peak sharpening after annealing can be explained on the basis of phonon confinement theory [28, 29], which predicts that the peaks will sharpen as the crystallites get bigger. This, for the first time, shows that the Raman spectra can be used in studied films for the determination of the film crystallinity in Cr_2AlC .

The third area shows peaks D and G typical for carbon bonding (marked as peaks 4a and 4b, respectively). For an as-deposited sample only the D band with low intensity is visible but, after annealing, the intensity increases and the additional G band appears. These differences in Raman spectra for as-deposited and annealed samples suggest that there is significant phase transformation as a result of the annealing process in the surface region and some carbon precipitation occurs in accordance with the known instability of transitional metal carbides [30].

In summary, we have shown that the ternary alloy of composition Cr_2AlC which, when crystalline, belongs to the class of so-named MAX-phases was deposited by ion beam sputtering onto unheated Si substrates. The as-deposited films have very small crystallites. Crystallisation can be achieved by annealing in air and, annealing in air at 700°C leads to crystallite growth to 32.3 nm. There is then also partial oxidation of the film which has been investigated by WDX spectroscopy with spectra taken at different electron beam energies. It

is possible to estimate, assuming fully stoichiometric oxides, that the oxide layer is less than 5% of total film thickness after annealing at 700 °C in air for 30 min. This indicates the possibility that films can be crystallized in air without significant oxygen contamination. Film structure and crystallisation have also been analysed by Raman spectroscopy. This is the first time that changes in Raman spectra in Cr₂AlC have been correlated with crystallite size and we have observed that MAX-phase related peaks become sharper for bigger crystallites.

Acknowledgements

The financial support of the UK Engineering and Physical Sciences Research Council (EP/G033471/1) for this programme and for the MMU Analytical Microscope (EP/F056117/1) is gratefully acknowledged.

References

- [1] G.L. Miller, F.G. Cox, *Journal of the Less Common Metals*, 2 (1960) 207-222.
- [2] P. Kofstad, S. Espevik, *Journal of the Less Common Metals*, 12 (1967) 117-138.
- [3] W. Jeitschko, H. Nowotny, F. Benesovsky, *Monatsh. Chem.*, 94 (1963) 332-333.
- [4] H. Nowotny, H. Boller, O. Beckmann, *Journal of Solid State Chemistry*, 2 (1970) 462-471.
- [5] M.W. Barsoum, T. El-Raghy, *J. Am. Ceram. Soc.*, 79 (1996) 1953-1956.
- [6] M.W. Barsoum, *Progress in Solid State Chemistry*, 28 (2000) 201-281.
- [7] H.B. Zhang, Y.W. Bao, Y.C. Zhou, *J. Mater. Sci. Technol.*, 25 (2009) 1-38.
- [8] P. Eklund, M. Beckers, U. Jansson, H. Högberg, L. Hultman, *Thin Solid Films*, 518 (2010) 1851-1878.
- [9] M.W. Barsoum, M. Radovic, *Annu. Rev. Mater. Res.*, 41 (2011) 195-227.
- [10] J.-P. Palmquist, U. Jansson, T. Seppanen, P.O.Å. Persson, J. Birch, L. Hultman, P. Isberg, *Appl. Phys. Lett.*, 81 (2002) 835.
- [11] C. Walter, D.P. Sigumonrong, T. El-Raghy, J.M. Schneider, *Thin Solid Films*, 515 (2006) 389-393.
- [12] D.P. Sigumonrong, J. Zhang, Y. Zhou, D. Music, J.M. Schneider, *J. Physics D: Appl. Phys.*, 42 (2009) 185408.
- [13] O. Wilhelmsson, P. Eklund, H. Hogberg, L. Hultman, U. Jansson, *Acta Materialia*, 56 (2008) 2563-2569.
- [14] P. Eklund, M. Bagnet, V. Mauchamp, S. Dubois, C. Tromas, J. Jensen, L. Piraux, L. Gence, M. Jaouen, T. Cabioch, *Phys. Rev. B*, 84 (2011) 075424.
- [15] J.M. Schneider, D.P. Sigumonrong, D. Music, C. Walter, J. Emmerlich, R. Iskandar, J. Mayer, *Scripta Materialia*, 57 (2007) 1137-1140.
- [16] Q.M. Wang, A. Flores Renteria, O. Schroeter, R. Mykhaylonka, C. Leyens, W. Garkas, M. to Baben, *Surface and Coatings Technology*, 204 (2010) 2343-2352.
- [17] J.J. Li, M.S. Li, H.M. Xiang, X.P. Lu, Y.C. Zhou, *Corrosion Science*, 53 (2011) 3813-3820.
- [18] J. Frodelius, P. Eklund, M. Beckers, P.O.Å. Persson, H. Högberg, L. Hultman, *Thin Solid Films*, 518 (2010) 1621-1626.
- [19] H. Högberg, L. Hultman, J. Emmerlich, T. Joelsson, P. Eklund, J.M. Molina-Aldareguia, J.P. Palmquist, O. Wilhelmsson, U. Jansson, *Surface and Coatings Technology*, 193 (2005) 6-10.
- [20] V. Vishnyakov, J. Lu, P. Eklund, *J.S. Colligon, Vacuum*, 93 (2013) 56-59.

- [21] M. Hopfeld, R. Grieseler, T. Kups, M. Wilke, P. Schaaf, *Adv. Eng. Mat.*, 15 (2013) 269-275.
- [22] V.M. Vishnyakov, V.I. Bachurin, K.F. Minnebaev, R. Valizadeh, D.G. Teer, J.S. Colligon, V.V. Vishnyakov, V.E. Yurasova, *Thin Solid Films*, 497 (2006) 189-195.
- [23] L. Lutterotti, D. Chateigner, S. Ferrari, J. Ricote, *Thin Solid Films*, 450 (2004) 34-41.
- [24] K. Syassen, *Datlab*, version 1.38XP MPI/FKF Stuttgart, Germany, (2005).
- [25] J.E. Spanier, S. Gupta, M. Amer, M.W. Barsoum, *Phys. Rev. B*, 71 (2005) 012103.
- [26] F.D. Hardcastle, I.E. Wachs, *J. Mol. Cat.*, 46 (1988) 173-186.
- [27] Z.M. Sun, R. Ahuja, S. Li, J.M. Schneider, *Appl. Phys. Lett.*, 83 (2003) 899.
- [28] I.H. Campbel, P.M. Fauchet, *Solid. State Commun.*, 58 (1986) 739-745.
- [29] N. Mahdjoub, N. Allen, P. Kelly, V. Vishnyakov, *Journal of Photochemistry and Photobiology A: Chemistry*, 211 (2010) 59-64.
- [30] H.W. Hugosson, U. Jansson, B. Johansson, O. Eriksson, *Chem. Phys. Lett.*, 333 (2001) 444-450.

Figure captions

Fig.1 Typical X-Ray spectra from Cr₂AlC sample analysed by Energy Dispersive Spectroscopy (EDX).

Fig.2. WDX spectra of as deposited and annealed-in-air samples (shown as lines with symbols). Lines without symbols belong to the oxygen K_α line deconvoluted from the spectra.

Fig.3. GIXRD patterns of as-deposited samples and samples annealed for 30 minutes in air or in vacuum at 700°C.

Fig.4. Raman spectra for Cr₂AlC MAX phases comparing as-deposited and annealed samples. 1a-1d peak range is typical for 211 MAX phases, peak 2 is for chromium oxides, 3a and 3b are for vibration in chromium carbide, 4a and 4b are for carbon-to-carbon bonds.

Table captions

Table 1: Lattice parameters and average crystal size for the investigated samples

Table 2. Peak position values for as-deposited and annealed samples and the literature values for MAX phases.

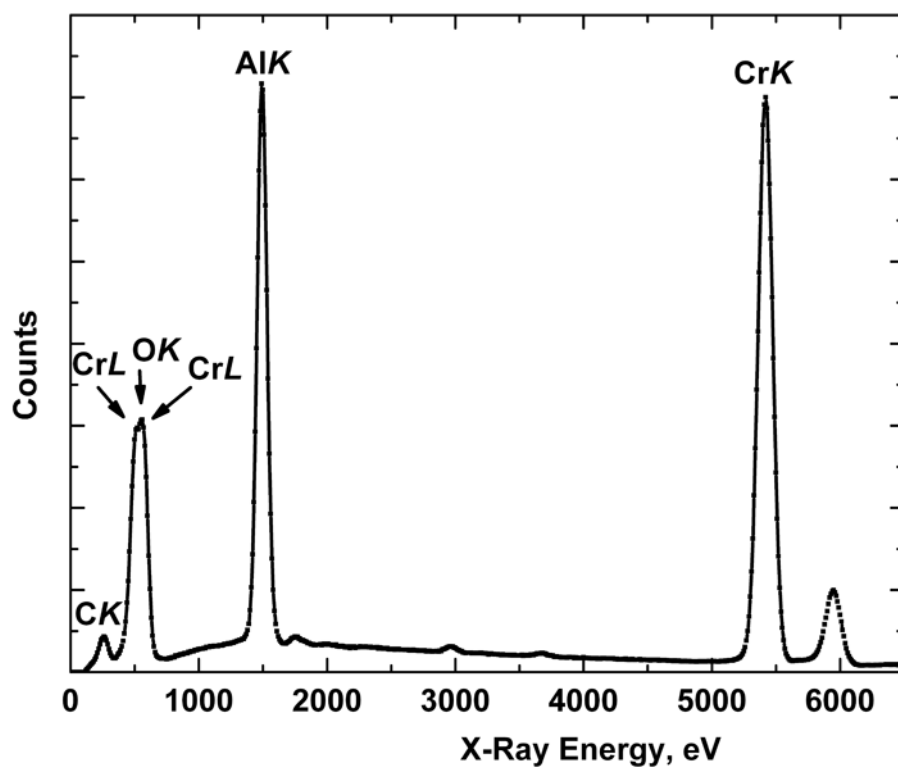


Fig.1 Typical X-Ray spectra from Cr_2AlC sample as analysed by Energy Dispersive Spectroscopy (EDX).

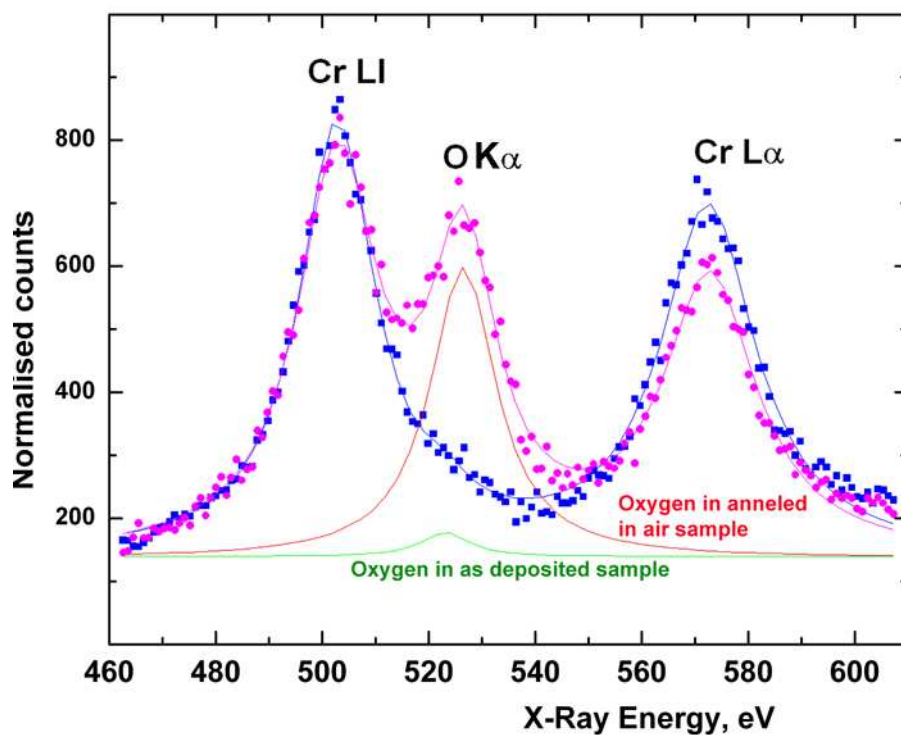


Fig.2. WDX spectra of as deposited and annealed-in-air samples (shown as lines with symbols). Lines without symbols belong to the oxygen K_α line deconvoluted from the spectra.

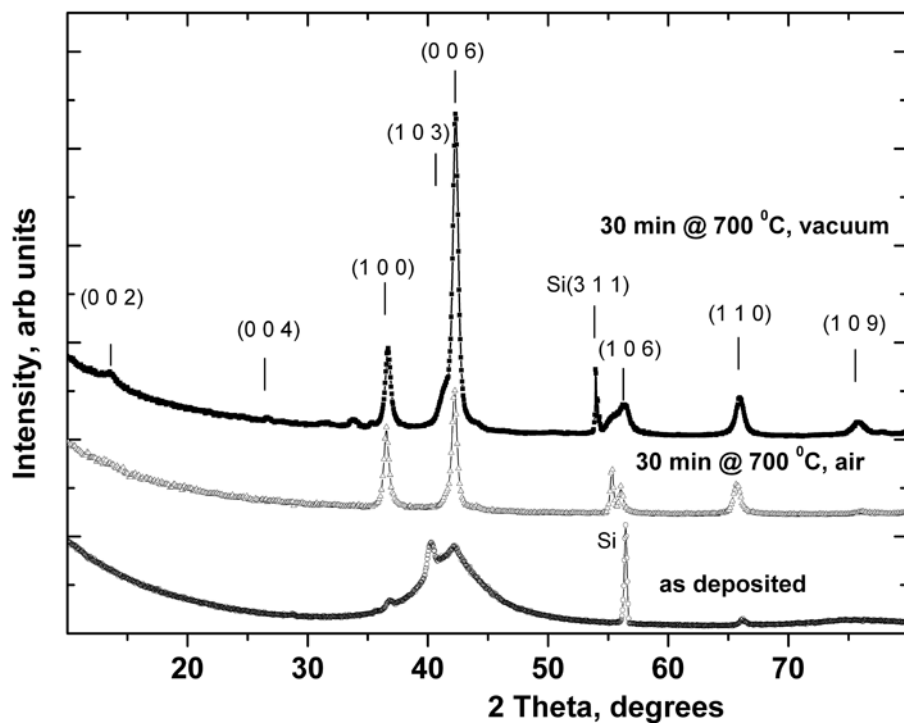


Fig.3. GIXRD patterns of as-deposited samples and samples annealed for 30 minutes in air or in vacuum at 700°C.

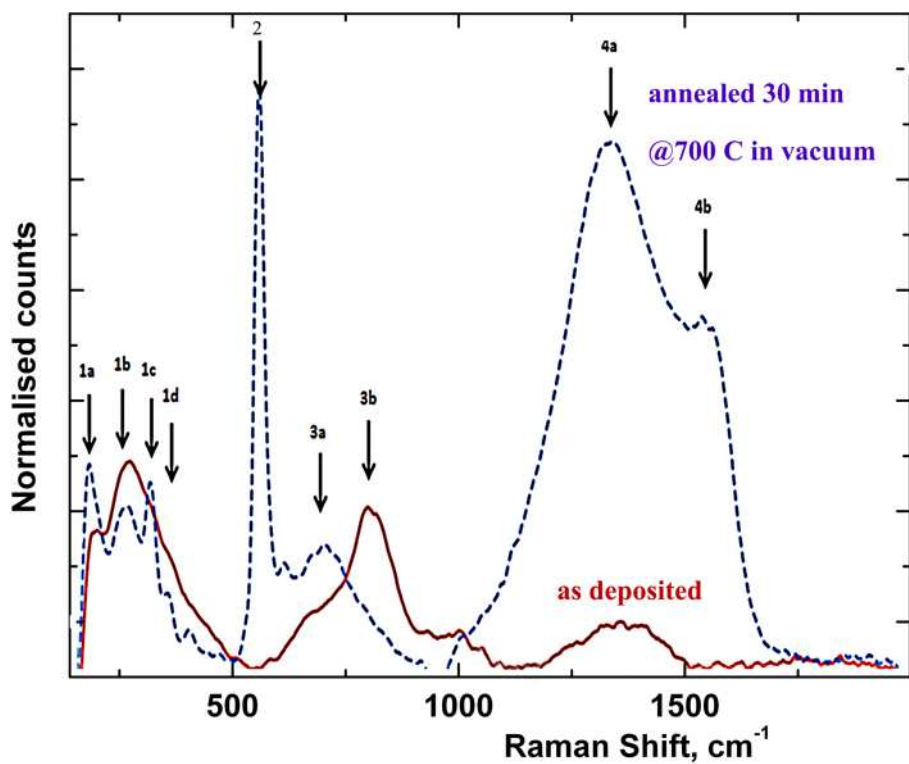


Fig.4. Raman spectra for Cr₂AlC MAX phases comparing as-deposited and annealed samples. 1a-1d peak range is typical for 211 MAX phases, peak 2 is for chromium oxides, 3a and 3b are for vibration in chromium carbide, 4a and 4b are for carbon-to-carbon bonds.

Table 1: Lattice parameters and average crystal size for the investigated samples

	Lattice parameters			Crystal size
	a (Å)	c (Å)	V (nm ³)	(nm)
as deposited on cold substrate	2.82±0.005	13.6±0.017	0.382	6.6±0.8
as deposited on substrate at 380 °C	2.83±0.001	12.86±0.014	0.364	14.2±3.2
Annealed in vacuum 30 min @ 700 °C	2.84±0.009	13.15±0.013	0.373	32.3±2.8
Annealed in air 30 min @ 700 °C	2.83±0.008	12.97±0.019	0.367	23.6±2.2

Table 2. Peak position values for as-deposited and annealed samples and the literature values for MAX phases.

Peak no.	Raman peak positions (cm ⁻¹)								
	1a	1b	1c	1d	2	3a	3b	4a	4b
as-deposited	176.3	251.3	*	347.4	-	675.2	808.7	1364.8	-
annealed at 30 min @700°C in vacuum	169.5	254.2	304	347.5	552.5	696.6	826.3	1354.1	1571.9
Literature values [24-26]	150.9	246.3	*	339.2	544	n/a	n/a	n/a	n/a